

Water balance components estimation under scenarios of land cover change in the Veia Catchment, West Africa

Article

Accepted Version

Larbi, I., Obuobie, E., Verhoef, A., Julich, S., Feger, K.-H., Bossa, A. Y. and Macdonald, D. (2020) Water balance components estimation under scenarios of land cover change in the Veia Catchment, West Africa. *Hydrological Sciences Journal*, 65 (13). pp. 2196-2209. ISSN 2150-3435 doi: <https://doi.org/10.1080/02626667.2020.1802467> Available at <https://centaur.reading.ac.uk/91306/>

It is advisable to refer to the publisher's version if you intend to cite from the work. See [Guidance on citing](#).

To link to this article DOI: <http://dx.doi.org/10.1080/02626667.2020.1802467>

Publisher: Taylor and Francis

All outputs in CentAUR are protected by Intellectual Property Rights law, including copyright law. Copyright and IPR is retained by the creators or other copyright holders. Terms and conditions for use of this material are defined in the [End User Agreement](#).

www.reading.ac.uk/centaur

CentAUR

Central Archive at the University of Reading

Reading's research outputs online



Water balance components estimation under scenarios of land cover change in the Vea Catchment, West Africa

Journal:	<i>Hydrological Sciences Journal</i>
Manuscript ID	HSJ-2019-0402.R2
Manuscript Type:	Original Article
Date Submitted by the Author:	30-Apr-2020
Complete List of Authors:	Larbi, Isaac; University of Abomey-Calavi Faculty of Science and Technology, climate change and water resources Obuobie, Emmanuel; CSIR-Water Research Institute, Verhoef, Anne; University of Reading, Julich, Stefan; TU Dresden Feger, Karl-Henze; Technische Universität Dresden Bossa, Aymar; University of Abomey-Calavi Faculty of Science and Technology Macdonald, David; British Geological Survey - Wallingford Office
Keywords:	Water balance components, Vea catchment, SWAT modeling, land cover change scenarios

SCHOLARONE™
Manuscripts

1
2
3
4 **1 Water balance components estimation under scenarios of land cover**
5
6 **2 change in the Vea Catchment, West Africa**
7
8

9 *Isaac Larbi¹, Emmanuel Obuobie², Anne Verhoef³, Stefan Julich⁴, Karl-
10 Henz Feger⁴, Aymar Yaovi Bossa⁵ and David M. J. Macdonald⁶
11

12
13 *1Climate Change and Water Resources, West African Science Service Centre on*
14 *Climate Change and Adapted Land Use (WASCAL), Universite d'Abomey Calavi,*
15 *Cotonou, Benin*
16

17 *2Water Research Institute, CSIR, Accra, Ghana;*
18

19 *3 Department of Geography and Environmental Science, University of Reading, UK*
20

21 *4 Institute of Soil Science and Site Ecology, Technische Universität Dresden, Germany*
22

23 *5National Water Institute, University of Abomey Calavi, 01 BP5, Cotonou, Benin*
24

25 *6 British Geological Survey, Wallingford, Oxfordshire, UK*
26

27
28 *Corresponding author: larbi.i@edu.wascal.org
29
30
31
32
33
34
35
36
37
38
39
40
41
42
43
44
45
46
47
48
49
50
51
52
53
54
55
56
57
58
59
60

15 **Water balance components estimation under scenarios of land cover** 16 **change in the Veia Catchment, West Africa**

17 **Abstract** The need for a detailed investigation of the Veia catchment water balance
18 components cannot be overemphasized due to its accelerated land cover dynamics
19 and its associated impacts on the hydrological processes. This study assessed the
20 possible consequences of land use change scenarios (i.e. business as usual (BAU)
21 and afforestation, for the year 2025) compared to 2016 baseline, on the Veia
22 catchment's water balance components using the Soil and Water Assessment Tool
23 (SWAT) model. The data used include daily climate and discharge, soil and land
24 use/land cover maps. The results indicate that the mean annual water yield may
25 increase by 9.1% under BAU scenario, but decrease by 2.7% under afforestation
26 scenario. Actual evapotranspiration would decrease under BAU scenario but
27 increase under afforestation scenario. Groundwater recharge may increase under
28 both scenarios, but more pronounced under the afforestation scenario. These
29 outcomes highlights the significance of land cover dynamics in water resource
30 management and planning at the catchment.

31 **Keywords:** Water balance components; Veia catchment; SWAT modeling; land
32 cover change scenarios

33 **1 INTRODUCTION**

34 Although freshwater constitutes less than 3% of the world's water resources, it forms an
35 important part of all terrestrial ecosystems. Concerns about the management of this
36 limited resource in river basins have been on the increase due to changes in climatic
37 conditions combined with anthropogenic influences (Jones *et al.* 2015, Zhang *et al.* 2008).
38 Effective catchment management requires a thorough knowledge of the hydrological
39 processes and their spatial distribution over the catchment (Wang *et al.* 2015). Land
40 use/land cover (LULC) change is one of the main human induced activities which
41 potentially impacts hydrology and water resources by affecting different hydrological
42 processes and stores in the catchment (Bhaduri *et al.* 2000, Tang *et al.* 2005, Stonestrom
43 *et al.* 2009). The changes in LULC have a direct and significant impact on the amount of
44 evapotranspiration, surface runoff and groundwater recharge driven by infiltration during
45 and after precipitation events (Doerr *et al.* 2000, Wei *et al.* 2013).

46 In the past decades, modelling of hydrological response to the changes in LULC
47 has become increasingly important. The changes in LULC, such as the conversion of
48 forest to agriculture and urban areas, have accelerated the rate of surface runoff and also
49 affected other water balance components (Costa *et al.* 2003, Jat *et al.* 2009, Awotwi *et al.*
50 2014). A study conducted by Mwangi *et al.* (2016) on agroforestry impact on the
51 hydrology of the Mara river basin, East Africa found a decrease in water yield (surface
52 runoff, groundwater flow and lateral flow) due to the increase in tree cover. A similar
53 study by Mango *et al.* (2010) investigated the hydrological response of the Mara River
54 basin to land use change and found a decrease in river baseflow and average streamflow
55 due to the conversion of forest to agriculture and grassland. Using a semi-distributed

1
2
3 56 hydrological modelling approach, Awotwi *et al.* (2014) estimated that the conversion of
4 57 savanna (30.2%) and grassland (56.2%) to cropland caused a decrease in surface runoff
5 58 and groundwater during the period from 1990 to 2006 in the White Volta basin (WVB)
6 59 in West Africa. The above studies confirm that the water resources are under threat from
7 60 the effects of LULC change.
8
9

10 61 In the past decades, several hydrological models have been developed to simulate
11 62 the water balance of catchments, especially in data scarce regions. These catchment
12 63 models are generally applied for water balance assessments (Ghoraba 2015, Vilaysane *et*
13 64 *al.* 2015, Bansode and Patil, 2016, Yin *et al.* 2016) or climate/land use change impact
14 65 assessments (Zhang *et al.* 2008, Mohamed, 2010, Palazzoli *et al.* 2015). Among these
15 66 models, the physically based semi-distributed Soil and Water Assessment Tool (SWAT)
16 67 model is a well-established model for estimation of water balance components, as well as
17 68 for the analysis of the impact of land management practices on water, sediment and
18 69 agricultural chemical yields in large complex catchments (Arnold *et al.* 1993). The
19 70 SWAT model is one of the most widely used hydrologic models and has been applied in
20 71 the USA, China, Europe, South Asia and Africa (Abbaspour *et al.* 2009). Hydrological
21 72 models face challenges in terms of data requirements, spatial heterogeneity of basin
22 73 characteristics, and how to represent complex terrestrial systems by model equations.
23 74 SWAT is capable of overcoming some of these challenges (Gassman *et al.* 2007). The
24 75 model has been used for a wide range of applications such as those relating to hydrology,
25 76 including hydrological climate change impact studies (Gassman *et al.* 2007). In West
26 77 Africa, a number of studies (Schuol and Abbaspour, 2007, Obuobie 2008, Kasei 2010,
27 78 Kankam-Yeboah *et al.* 2013, Bossa *et al.* 2014) evaluated the SWAT model favourably
28 79 in the context of water balance simulation. For example, Obuobie (2008) applied the
29 80 SWAT model in the WVB to simulate the water balance components and found a good
30 81 agreement between simulated and observed annual discharge, surface runoff and
31 82 baseflow with a coefficient of determination (R^2) and Nash-Sutcliffe model Efficiency
32 83 (NSE) both greater than 0.80. Other studies, such as Awotwi *et al.* (2015), also confirmed
33 84 that the SWAT model was able to simulate reliably the hydrology of the WVB, hence the
34 85 use of SWAT in our study.
35
36

37 86 Fresh water availability and distribution have been declining over time partly due
38 87 to changes in LULC and population growth. Studies such as Braimoh and Vlek (2004),
39 88 Forkuor (2014), and Batuuwie (2015), have all reported substantial changes in LULC
40 89 over recent years within the Volta basin, where the Veia catchment is located. The study
41 90 by Batuuwie (2015) indicated that a significant portion of natural vegetation cover in the
42 91 WVB, has been lost over the years partly due to human activities. Similarly, a study by
43 92 Larbi *et al.* (2019) indicated the conversion of forest/mixed vegetation to cropland as the
44 93 dominant LULC from 1990 to 2016 in the Veia catchment. Their projection of LULC
45 94 predicted continuous expansion of cropland at the expense of forest/mixed vegetation
46 95 with an estimated decrease of non-agricultural vegetation of 4.5% between 2016 and
47 96 2025, under business as usual scenario (Larbi *et al.* 2019). This unfavorable situation of
48 97 LULC change has heightened the need for afforestation and the protection of forest
49 98 reserves in most river basins in Ghana such as the Veia catchment. There is however a
50 99 tradeoff between afforestation and surface water resources. For example, forest improves

1
2
3 100 water quality and enhances infiltration but uses more water, causing higher
4 101 evapotranspiration and lower runoff (Yira *et al.* 2017). Hence, there is an urgent need for
5 102 catchment scale water balance information since the changes in LULC have been shown
6 103 to alter the hydrological processes of many river basins (Stonestrom *et al.* 2009, Mwangi
7 104 *et al.* 2016). In the study region, although Awotwi *et al.* (2014) undertook a broader scale
8 105 study of LULC change impact on water resources on the entire White Volta basin, little
9 106 is known at the local scale (e.g. for a sub-catchment such as the Vea). The previous large
10 107 scale study of LULC change impacts on water balance have used coarse resolution data
11 108 for land use, digital elevation model (DEM) and soil, which may ignore or over-simplify
12 109 landscape characteristics that relate to the hydrology of the Vea catchment. Having a
13 110 higher resolution DEM and LULC data provides better details for drainage, slope and
14 111 related land use types for small scale catchments. According to the study by Sivasena and
15 112 Janga (2015), the accuracy of sub-catchments decreases with coarse resolution data, and
16 113 this affects the generated runoff at the HRU level within each sub-catchment. There is
17 114 also the issue of data scarcity and uneven distribution of climate stations in the catchment
18 115 that hampers spatio-temporal studies of the various components of the water balance
19 116 (Ibrahim *et al.* 2015). The issue of data scarcity is a challenge in Ghana, hence the need
20 117 to rely on high-resolution satellite-based climate products for hydrological studies.

21
22
23
24
25
26
27 118 Moreover, in the Vea catchment there is a proposed initiative to increase the
28 119 number of small dams or dugouts with the aim of ensuring all year round crop production.
29 120 This initiative as a result may increase cropland area in the future and also affect other
30 121 land use types, which would eventually alter the water balance of the catchment. Given
31 122 the reviewed impacts of LULC change on hydrological processes in Ghana, the need for
32 123 a detailed investigation of the Vea catchment water balance components cannot be
33 124 overemphasized due to its accelerated land cover dynamics and its associated impacts on
34 125 the hydrological processes. This study assessed the possible consequences of land use
35 126 change scenarios (i.e. business as usual and afforestation, for the year 2025) compared to
36 127 2016 baseline, on the Vea catchment's water balance components (actual
37 128 evapotranspiration, surface runoff, water yield and groundwater recharge) using the Soil
38 129 and Water Assessment Tool (SWAT) model. The specific objectives of this study are to:
39 130 (i) apply the SWAT model to simulate the water balance components of the data-scarce
40 131 Vea catchment using both weather station and high-resolution (5km) gridded
41 132 precipitation data; and (ii) estimate the impact of business-as-usual (BAU) and
42 133 afforestation scenarios of land cover change on the water balance components. The BAU
43 134 scenario deals with the projection of the LULC pattern based on expansion in cropland
44 135 and grassland at the expense of forest/mixed vegetation, while the afforestation scenario
45 136 deals with the by limiting cropland expansion into the forested areas and increasing
46 137 natural vegetation (forest cover and grassland). The study provides information on the
47 138 present water balance components of the catchment and the implication of different
48 139 scenarios of LULC change on the future water resources which are relevant to decision
49 140 makers for a sustainable management of the land and water resources of the Vea
50 141 catchment.
51 142

143 2 MATERIALS AND METHODS

144 2.1 Study area

145 The Veia catchment, with an area of 306 km², is one of the three focal experimental
146 catchments of the West African Science Service Center on Climate Change and Adapted
147 Land Use (WASCAL); it is located within the White Volta basin (Figure 1). The Veia
148 catchment covers mainly the Bongo and Bolgatanga districts in the Upper East region of
149 Ghana and lies between latitudes 10°30' - 11°08' N and longitudes 0° 59' - 0° 45' W. The
150 catchment lies mainly in Ghana, with a small northern portion located in the south-central
151 part of Burkina Faso. The climate of the catchment is controlled by the movement of the
152 Inter-Tropical Discontinuity (ITD) that dominates the climate of the entire West African
153 region (Obuobie 2008). Located in a semi-arid agro-climatic zone, the catchment covers
154 three agro-ecological zones: the Savanna and Guinea Savanna zones in Ghana, and north
155 Sudanian Savanna zone in Burkina Faso (Forkuor 2014). It is characterized by a uni-
156 modal rainfall regime from April/May to October with a mean annual rainfall of 957 mm
157 which normally peaks in August, and a very high potential evapotranspiration with a
158 mean annual value ranging from 1650mm to 1950mm (Limantol *et al.* 2016, Larbi *et al.*
159 2018). It is characterized by fairly low relief with elevation ranging between 89 m and
160 317m (Figure 1) and mainly dominated by cropland followed by grassland interspersed
161 with shrubs and trees, and woodland (closed/open) (Figure 2 and Table 3). The dominant
162 soil type in the Veia catchment is lixisols (90%) while vertisols (8%) and cambisols (2%)
163 occur in relatively smaller proportions (Figure 2). The catchment also contains a
164 considerable number of wetlands and valleys, and contains the Veia dam and many small
165 dams (used for irrigation and animal watering) and wells/pumps, resulting in a complex
166 hydro-ecological system. Agriculture (rain-fed and irrigated), which includes the
167 cultivation of annual crops such as: beans, rice, sorghum, millet, and groundnuts is one
168 of the main sources of income for many of the rural people in the catchment. The
169 construction of the Veia irrigation project in the 1980s for irrigation farming and provision
170 of potable water to the surrounding communities has led to changes in LULC in the
171 catchment (Adongo *et al.* 2014).

172
173 **Figure 1** Location of the Veia catchment within the White Volta Basin, as well as the
174 topography, weather and hydrological measurement stations in the Veia catchment, after
175 Larbi *et al.* (2018).

176 2.2 Data collection and preparation

178 The SWAT model requires a Digital Elevation Model (DEM), daily
179 meteorological data, soil and land use/cover map and management as input data. The
180 characteristics of the datasets used for this study and their sources are listed in **Table 1**.
181 Meteorological observations for the Veia catchment were taken mainly from the
182 Bolgatanga and Veia climate stations maintained by WASCAL (Figure 1). Due to the
183 sparse distribution of climate stations throughout the catchment, daily precipitation data
184 from the Climate Hazards Group InfraRed Precipitation with Station (CHIRPS) data were

1
2
3 185 used to complement the observed data. CHIRPS combines 0.05° resolution satellite
4 186 imagery with in-situ station data to create gridded rainfall time series (Funk et al., 2015).
5 187 The CHIRPS data have been demonstrated to reproduce well both the seasonal and annual
6 188 rainfall pattern of the Vea catchment, with validation resulted in a very high correlation
7 189 coefficient ($r = 0.99$), and a Nash–Sutcliffe efficiency of 0.9, indicating that the CHIRPS
8 190 precipitation data can be employed in this study (Larbi *et al.* 2018). The CHIRPS daily
9 191 precipitation data were extracted for the various grid locations within the Vea catchment
10 192 (Figure 1). These gridded locations (Figure 1, right) were selected to represent the three
11 193 agro-ecological zones namely; the Savanna zone (GRID3, GRID 4, GRID 5, GRID 6,
12 194 GRID 7 and GRID 8), the Guinea Savanna (GRID 9, GRID 10, GRID 11 and GRID 12)
13 195 and the north Sudanian Savanna zone (GRID 1 and GRID 2) in the study area (Larbi *et*
14 196 *al.* 2018). Missing records (less than 10%) in the Vea and Bolgatanga stations data were
15 197 filled with the CHIRPS precipitation data and the 0.5° resolution daily minimum and
16 198 maximum temperature data from the NASA Langley Research Center (LaRC) POWER
17 199 project (Stackhouse *et al.* 2018). The LULC map (Figure 2) was obtained from the
18 200 maximum likelihood algorithm classification of Landsat image of the year 2016 with the
19 201 details of the LULC classification found in Larbi *et al.* (2019). Tables 2 and Table 3 show
20 202 the various LULC types and the associated statistics.
21
22
23
24
25
26
27
28
29
30

31 **Figure 2** Land use/land cover (left), Soil (middle), and slope classes (right) maps of the
32 Vea catchment. Lixisols (Lf1-1a), vertisols (Vc1) and cambisols (Bv2)
33

34 **Table 1.** Datasets used within the SWAT modelling of the Vea Catchment and their
35 sources
36

37 **Table 2.** Land use/ land cover classification scheme used for the Vea Catchment after
38 Larbi et al. (2019)
39

40 **Table 3.** Distribution of 2016 land use/cover classes within the Vea catchment (Larbi *et*
41 *al.* 2019)
42
43
44

45 217 **2.3 Hydrological Modelling**

46 218 **2.3.1 Hydrological components of SWAT Model**

47
48 219 The SWAT model is an eco-hydrological model developed to simulate the quantity and
49 220 quality of surface water and groundwater, and predict the environmental impact of land
50 221 management practices, land use and climate change (Arnold *et al.* 1998, Cornelissen *et*
51 222 *al.* 2013). SWAT is useful in modelling ungauged catchment and it simulates the
52 223 catchment by first dividing it into sub-catchments, and then into homogenous units that
53 224 consist of uniform land use, soil and slope characteristics called Hydrologic Response
54 225 Units (HRUs) (Neitsch *et al.* 2005). In SWAT, the quantification of the hydrological cycle
55 226 components is based on the water balance equation and is expressed mathematically as:
56
57
58
59
60

$$SW_t = SW_o + \sum_{i=1}^t (R_{day} - Q_{surf} - ET - W_{seep} - Lt_{flow} - Q_{gw}) \quad (1)$$

where SW_t is the final soil profile water content (mm); SW_o is the initial soil water content on day i (mm); R_{day} , Q_{surf} , ET , W_{seep} , Lt_{flow} and Q_{gw} are the daily amounts (mm) of rainfall, surface runoff, actual evapotranspiration, percolation, lateral flow, and the groundwater flow on day i , respectively. The water yield component, considered in this study consists of the contributions from surface runoff, lateral flow and groundwater flow to stream flow.

In this study, the Soil Conservation Service (SCS) curve number equation (SCSD, 1986) was used to compute the Q_{surf} SWAT. The Lt_{flow} which is the lateral movement of water in the soil profile was simulated using the kinematic storage model method of Sloan and Moore (Sloan and Moore 1984), which is based on mass continuity equation. The potential evapotranspiration (PET) in this study was estimated using the Hargreaves method (Hargreaves and Samani, 1985), which requires only air temperature as input data. The model then computes ET once PET is determined. The groundwater recharge to the shallow aquifer is simulated by SWAT using equation 2.

$$W_{rchg,sai} = (1 - \exp[-1/\delta_{gw}]) \cdot W_{seep} + \exp[-1/\delta_{gw}] \cdot W_{rchg,sai-1} \quad (2)$$

where $W_{rchg,sai}$ and $W_{rchg,sai-1}$ are the amount of recharge from the soil profile entering the shallow aquifer on day i and $i-1$ (mm); and δ_{gw} is delay time or drainage time (days).

The Veia catchment was delineated into 52 sub-catchments with an estimated total surface area of about 306 km² using the 30m DEM. The 2016 LULC map and soil map were used to define the HRUs of the catchment. The multiple HRUs definition option was used to further sub-divide the Veia catchment into 331 HRUs. The model was run for the period of 1990-2017; and the first three years (1990-1992) were used as model spin up period. For a detailed description of how SWAT model simulate the water balance components and the model setup, readers may refer to SWAT documentation by Neitsch *et al.* (2005), and SWAT user guide by Winchell *et al.* (2013).

2.3.2 Model sensitivity analysis, calibration and evaluation of prediction performance

The SWAT model sensitivity analysis, calibration and validation were performed via the interface of SWAT-CUP using the Sequential Uncertainty Fitting version 2 (SUFI-2) procedure (Abbaspour *et al.* 2009). The superior capability for calibration and uncertainty analysis has been demonstrated by various studies, e.g. Shawul *et al.* (2013), Abbaspour *et al.* (2009). The sensitivity analysis was performed by testing a total of 13 parameters (Table 5) based on previous studies (Obuobie, 2008; Guug, 2017) and SWAT documentation recommendations (Neitsch *et al.* 2011). The SWAT model for the Veia catchment was calibrated manually as well as automatically based on the available daily observed discharge data similar to studies such as Kankam-Yeboah *et al.* (2013), and Dos Santos *et al.* (2018). The calibration was performed for the period (May 2014 to November 2014 and June 2015 to November 2015), and validation for the period (July to November 2013) at the Sumbrungu gauge station (Figure 1). Due to the limited length of the time series, and gaps within the observed discharge data, manual calibration was performed first based on the authors and experts knowledge of the catchment in order to

268 ensure that the various water balance components were within reasonable and/acceptable
 269 ranges. Moreover, SWAT applications literature in the region was used to support the
 270 manual calibration (e.g. Obuobie 2008, Kankam-Yeboah *et al.* 2013, Guug, 2017). The
 271 manual calibration was performed for a limited number of parameters, including SCS
 272 runoff curve number (CN₂), soil evaporation compensation factor (ESCO), and baseflow
 273 alpha factor (ALPHA_BF), by changing one parameter at a time and re-running the
 274 model. This choice of parameters was based on previous SWAT model runs for the area
 275 (Guug 2017). Manual calibration was then followed by automatic calibration to further
 276 tune the parameters (Table 5) for the entire catchment. The performance of the SWAT
 277 model was evaluated using Nash-Sutcliffe model efficiency (NSE; Eq. 3), coefficient of
 278 determination (R²; Eq. 4) and percentage bias (PBIAS; Eq. 5). PBIAS measures the
 279 average tendency of the simulated values to be larger or smaller than the observed. The
 280 optimal value of PBIAS is 0.0, with low-magnitude values indicating accurate model
 281 simulation. Negative values indicate overestimation, whereas positive values indicate
 282 underestimation. NSE is a commonly used statistic proposed by Nash and Sutcliffe (1970)
 283 and ranges from 1 to -∞ with a value of 1 corresponding to an exact fit between modelled
 284 and measured data. The R² gives information about the goodness of fit between the
 285 simulated data and the measured data. It ranges from 0 to 1, with 1 being the best fit
 286 between the simulated and the observed data; typically values greater than 0.5 are
 287 considered acceptable (Santhi *et al.* 2001). The model performance was rated according
 288 to the performance ratings proposed by Moriasi *et al.* (2007), which indicated that a
 289 hydrological model can be considered satisfactory if NSE > 0.50, R² > 0.60, and PBIAS
 290 is within ±25% for streamflow.

$$291 \quad NSE = 1 - \frac{\sum_{i=1}^n (O_i - P_i)^2}{\sum_{i=1}^n (O_i - \bar{O})^2} \quad (3)$$

$$292 \quad R^2 = \left[\frac{\sum_{i=1}^n (O_i - \bar{O})(P_i - \bar{P})}{\left[\sum_{i=1}^n (O_i - \bar{O})^2 \right]^{0.5} \left[\sum_{i=1}^n (P_i - \bar{P})^2 \right]^{0.5}} \right]^2 \quad (4)$$

$$293 \quad PBIAS = \frac{\sum_{i=1}^n (O_i - P_i)}{\sum_{i=1}^n (O_i - \bar{O})} \times 100 \quad (5)$$

294 In these equations O_i are the measured discharge data; P_i are the simulated discharge
 295 data, whereas \bar{O} and \bar{P}_i are the mean of the measured and simulated data, respectively.

297 **2.4 Land cover change scenarios and water balance impact assessment**

298 The 2016 LULC map and the two LULC change scenarios (BAU and afforestation)
 299 (Figure 3) used in this study were produced by Larbi *et al.* (2019). The 2016 LULC map
 300 was based on Maximum Likelihood algorithm classification of the 30m resolution
 301 Landsat image with an overall accuracy of 88%. This was adopted as a baseline in order
 302 to understand and obtain information on the current hydrological status at the Vea
 303 catchment. The two scenarios maps were produced using the Markov chain in the Land
 304 Change modeller. The Markov chain calculates how much land transition occurs from
 305 one class to another from time t_0 to t_1 in each transition based on the historical rate of
 306 LULC changes that occurred (Eastman 2006, Olmendo *et al.* 2015). Based on the most

1
2
3 307 dominant transitions (grassland to cropland, forest/mixed vegetation to cropland, and
4 308 forest/mixed vegetation to grassland) that occurred at the Vea catchment between the
5 309 period 1990 and 2016, the transition potential maps were produced using the Multi-Layer
6 310 Perceptron (MLP) neural network algorithm at an accuracy rate of 85% (Larbi *et al.*
7 311 2019). The BAU scenario map was produced based on the probability matrix generated
8 312 from the transition potential maps. In the case of afforestation scenario, the probability
9 313 matrix for the forest/mixed vegetation, grassland and cropland were modified based on
10 314 the definition of the afforestation scenario, while the other LULC types were assumed to
11 315 be maintained till the 2025. Table 4 shows the statistics for the 2016 LULC map and
12 316 projections for the two LULC scenarios. Under the BAU scenario, cropland and grassland
13 317 areas are projected to increase in the year 2025 by 1.5% and 6.5%, respectively, while
14 318 forest/mixed vegetation shows a decrease of 4.5%. Under the afforestation scenario, the
15 319 forest/mixed vegetation and grassland showed an increase of 5.4% and 14.3%,
16 320 respectively, while cropland decreased by 20%. Detailed information on the 2016 LULC
17 321 mapping, LCM validation and the two land-use scenarios are available in Larbi *et al.*
18 322 (2019).

19 323 After calibration and validation of the SWAT model using the 2016 LULC map,
20 324 the impacts of the two LULC change scenarios on the water balance components were
21 325 simulated by driving the calibrated SWAT model with the 2025 BAU and afforestation
22 326 scenarios LULC datasets. The SWAT model was run for each scenario using the climate
23 327 for the period 1993-2017, and the results under each scenario was compared to the
24 328 corresponding water balance components (actual evapotranspiration, water yield and
25 329 groundwater recharge) values for the 2016 LULC condition.

26 330 **Table 4.** Current and 2025 LULC area statistics (in km²) in the Vea catchment
27 331

28 332 **Figure 3** The baseline and 2025 LULC change scenarios maps of the Vea catchment
29 333 (Larbi et al. 2019)
30 334

31 335 **3 RESULTS AND DISCUSSION**

32 336 **3.1 Sensitivity, calibration and validation of SWAT model**

33 337 A total of 13 parameters were selected and presented together with their final fitted values
34 338 for the stream flow simulation with the SWAT model (Table 5). Generally, hydrological
35 339 models are sensitive to parameters related to soil, weather, vegetation, land management,
36 340 and channels properties (Arnold *et al.*, 2000). The average slope steepness (HRU_SLP),
37 341 SCS runoff curve number (CN₂), baseflow alpha factor (ALPHA_BF), soil evaporation
38 342 compensation factor (ESCO) and the threshold water depth in the shallow aquifer for
39 343 return flow to occur (GWQMN) emerged as the most sensitive parameters for the Vea
40 344 catchment. Similar results were reported by a number of studies in the same region using
41 345 the SWAT model (Obuobie, 2008; Kankam-Yeboah *et al.* 2013; Guug, 2017). The
42 346 comparison between the observed and simulated daily stream flows for the SWAT model

1
2
3 347 calibration (2014 – 2015) and validation (2013) periods are shown in Figure 4 and Figure
4 348 5, respectively. The values for R^2 and NSE for the calibration period were 0.75 and 0.69
5 349 respectively, whereas for the validation periods 0.71 and 0.62 were found respectively.
6 350 The obtained PBIAS results for the calibration (10.3%) and validation (-18.5%) of the
7 351 SWAT model is in line with the range for model satisfaction proposed by Moriasi *et al.*
8 352 (2017) indicating that, a hydrological model can be considered as satisfactory if $NSE >$
9 353 0.50 , $R^2 > 0.60$, and PBIAS is within $\pm 25\%$ for streamflow. The obtained modelling
10 354 statistics results are also in line with calibration results of previous SWAT modelling
11 355 studies at the study region (e.g. Obuobie, 2008; Kankam-Yeboah *et al.* 2013, Awotwi *et*
12 356 *al.* 2014). In addition, the hydrological balances produced by the SWAT model in this
13 357 study are close to values found for small Sudanian catchments in the study region
14 358 (Oguntunde, 2004, Martin 2005, Ibrahim *et al.* 2015). The obtained modelling statistics
15 359 results therefore provide a reasonable support for the model's ability to describe water
16 360 balance components of the Veia catchment.
17
18
19
20
21
22

23 362 **Table 5.** Input parameters and bounds, sensitivity ranking and calibrated values by the
24 363 SWAT model for the Veia catchment
25 364

26 365 **Figure 4** Simulated vs. Observed daily discharge for *calibration* period (2014-2015) at
27 366 Sumbrungu gauge station, Veia Catchment
28
29
30

31 368 **Figure 5** Simulated vs. Observed daily discharge for *validation* period (2013) for
32 369 Sumbrungu gauge station, Veia Catchment
33
34
35

36 372 3.2 Mean annual and monthly water balance components analysis

37
38 373 The mean annual simulated water balance components from the baseline model run over
39 374 the period 1993-2017, as a proportion of the mean annual rainfall, are shown Figure 6.
40 375 The results show that 74.3% of the mean annual rainfall (954 mm) is lost to ET in the
41 376 catchment during the model simulation period (1993-2017). The water yield (WYLD)
42 377 which consist of surface runoff, groundwater flow and lateral flow constitutes about
43 378 13.5% of the rainfall (128 mm), of which Q_{surf} accounts for 8.6%, while Q_{gw} and L_{tflow}
44 379 accounts for 3.4% and 1.4%, respectively. The recharge to the shallow aquifer ($W_{rchg,sa}$)
45 380 is simulated to be 12.1% (115 mm). The results obtained from this study are also in line
46 381 with other previous studies such as Martin, 2005; Friesen *et al.*, 2005; Obuobie, 2008;
47 382 Guug, 2017. For example, a very high actual evapotranspiration (ET) within the range of
48 383 73-75%, runoff in the range of 10-17% and shallow aquifer recharge (7-13%) for the year
49 384 2003 were obtained by a study conducted by Martin (2005) using a simple spreadsheet-
50 385 based soil water balance method for Atankwidi catchment (a 275 km² sub-catchment of
51 386 the White Volta in northern Ghana) which is adjacent to the Veia catchment. Similarly,
52 387 Ibrahim *et al.* (2015) determined the water balance for the Veia catchment, from water
53 388 budget modeling using the GR2M model, for the period 1970–2000 and found that about
54
55
56
57
58
59
60

389 74.6% of the mean annual rainfall (980mm) constitutes actual evapotranspiration, with
 390 runoff and recharge constituting 11.9% and 12.9% of the annual rainfall, respectively.

391 In terms of mean monthly distribution of the simulated water balance components
 392 (Figure 7), it was found that potential evapotranspiration (PET) exceeds rainfall in most
 393 of the months except July, August and September, which record the highest monthly
 394 rainfall of 173 mm, 266mm and 175mm, respectively. The ET increases steadily as
 395 rainfall increases during the season and decreases as the season approaches the dry
 396 season. During the first 6-9 weeks from the rainfall onset month (April), the model
 397 simulates rainfall being entirely partitioned to by ET and the replenishment of soil
 398 moisture storage. The surface runoff therefore becomes important only after this first
 399 period of approximately 2 months; it peaks together with the water yield in the month of
 400 August when the rainfall is highest. It is worth mentioning that the wet season is from
 401 May to October but the water yield extends to December due to groundwater baseflow
 402 (also see Guug, 2017).

403

404 3.3 Water balance components distributions for the different land use/land cover 405 types

406 The analysis of simulated mean annual water balance components, at the catchment scale,
 407 under different land use/cover types show that the lowest average annual Q_{surf} is from
 408 forest/mixed vegetation, whereas the highest values occur on grassland followed by
 409 cropland (Table 6). Grassland which covers about 26.9% of the catchment, has a mean
 410 annual Q_{surf} of 100.3mm, followed by cropland with a Q_{surf} of 88.5 mm, whereas the
 411 lowest Q_{surf} of 56.2mm is found for forest/mixed vegetation. For cropland and grassland
 412 this is equivalent to ~ 10% of the rainfall, whereas for forest/mixed vegetation it is only
 413 ~ 6%. The actual evapotranspiration (ET) is simulated to be between 73-74% of rainfall,
 414 i.e. the differences between the 3 land uses are virtually negligible. The contribution of
 415 Q_{gw} to streamflow is simulated to be relatively high in forest/mixed vegetation (7.7%),
 416 follow by cropland (5.6%) but low in grassland (4%).

417

418 **Table 6.** Mean annual water balance components simulated by SWAT under different
 419 land use/cover types at catchment scale

420

421 3.4 Water balance components changes under land use scenarios

422 The SWAT simulated mean monthly and annual water balance components for the period
 423 1990-2017 under the two LULC scenarios (BAU and afforestation) were compared with
 424 those simulated for the 2016 LULC (baseline run) to explore their temporal (Table 7) and
 425 spatial pattern (Figure 9) in the Veia catchment. **At annual scale under BAU scenario
 426 described in section 2.4, the mean annual surface runoff, water yield and groundwater
 427 recharge increased by 18.7%, 9.1% and 15.3% respectively and ET decreased by 2.7%
 428 (Table 7). In contrast, the opposite impact on ET occurred under the afforestation**

scenario, which showed a slight increase in ET by 0.6%, whereas surface runoff and water yield decreased by 19.6% and 18% respectively, while groundwater recharge increased by 28.1%. At the monthly scale, for the BAU scenario, the ET decreased by 4.9% in the rainy season months (May-Oct.) and Q_{surf} and WYLD increased by 18.6% and 8.7% respectively (Figure 8). Similarly, the afforestation scenario shows a 7.8% decrease in ET, 23.1% decrease in Q_{surf} and 19.1% decrease in WYLD but an increased recharge by 21.4% in the peak period of the rainfall season (July-Sept). At the spatial scale under the BAU scenario as shown in Figure 9, the ET shows a decrease in most part of the catchment (Figure 9b), but water yield (Figure 9h) and surface runoff especially at the central part of the catchment (Figure 9d-9f) increased. Under afforestation scenario, ET increased in the north-central part of the catchment (Figure 9c) and surface runoff decreased at the southern and northern parts (Figure 9f). The water yield decreased considerably in the entire catchment with the highest value of 197mm (Figure 9i) while groundwater recharge increase occurred at the northern part of the catchment would occur (Figure 9L).

Table 7. Mean annual water balance components under 2016 and 2025 LULC change scenarios over the simulated period (1993-2017)

Figure 8 Mean monthly water balance components under different scenarios of land use change

Figure 9 SWAT Simulated mean annual water balance components under BAU and afforestation scenarios of land use change relative to the baseline (2016) LULC map

The Curve number (CN) method is used by the SWAT model to compute the surface runoff for each land use. From Table 5, the curve number for cropland, grassland and forest are 72.5, 73.5 and 69 respectively with an average catchment curve number of 71.5. Therefore, grassland had the highest surface runoff at the catchment based on the curve number, followed by cropland and forest/mixed vegetation. The conversion from cropland to forest/mixed vegetation would lead to a decrease in curve number at that area hence a decrease in surface runoff under afforestation scenario. Surface runoff constitute about 63% of the water yield, hence a subsequent decrease in water yield under afforestation scenario. On the other hand, when forest is converted to cropland and grassland under BAU scenario, the curve number for the area where the conversion took place would increase which would lead to an increase in surface runoff and water yield.

The plant canopy influences infiltration, surface runoff and evapotranspiration under the different land use types. When computing surface runoff in SWAT, the SCS curve number method lumps canopy interception in the term for initial abstraction. The maximum amount of water that can be held on the canopy for subsequent evaporation (interception) is a function of the leaf area index (LAI). According to Chen and Black (1992), LAI is an important modulator of ET and groundwater recharge. The maximum

1
2
3 473 LAI (BLAI) values (Table 5) for forest/mixed vegetation, cropland and grassland for the
4 474 Vea catchment as simulated by the SWAT model are 5, 3 and 2.5 m² m⁻², respectively,
5 475 indicating higher interception in forest followed by cropland and grassland.
6 476

7 477
8 478 Higher ET occurred in forest/mixed vegetation (720mm/yr), followed by cropland
9 479 (700.5mm/yr) and grassland (698.8mm/yr) as shown in Table 6. This is because ET is
10 480 partly dependent on transpiration, which is directly proportional to the surface area of
11 481 leaves (equivalent to the LAI) from which water vapour is released. According to Adane
12 482 et al. (2018), the conversion from cropland to forest/mixed vegetation leads to increased
13 483 rooting depth, and greater leaf area index, which together alter the water budget
14 484 considerably. Hence under the afforestation scenario, we would expect the actual
15 485 evapotranspiration to increase and while the opposite would occur under BAU scenario.

16 486
17 487 Rooting depth determines the maximum depth from which plants can access moisture in
18 488 the soil profile and it has substantial influence on groundwater recharge and actual
19 489 evapotranspiration. In SWAT, the maximum rooting depth (RDMX) values for each land
20 490 use type were 3 m for forest/mixed vegetation, 1 m for grassland and cropland (Table 5).
21 491 Under both scenarios of land use change, groundwater recharge increased: in the BAU
22 492 scenario, this occurred because although there was more surface runoff, the increased
23 493 area of grassland and cropland meant lower ET. In the afforestation scenario, there was a
24 494 greater infiltration rate which outweighed the increased ET. In addition, automatic
25 495 calibration of the SWAT model indicated that water loss at the catchment was more
26 496 influenced by evaporation than transpiration as indicated by the coefficients of plant
27 497 uptake and soil evaporation compensation factors which were found to be 0.02 and 0.42
28 498 respectively (Table 5). This means that the evaporation process is sustained from deeper
29 499 soil layers, through capillary rise, whereas the transpiration only receives very little
30 500 contribution from the deeper soil layers. The dominant soil type in the Vea catchment are
31 501 lixisols (90%); these are soils with subsurface accumulation of mainly kaolinitic clays,
32 502 whereas approximately 8% of the catchment is characterized by the presence of vertisols
33 503 (dominated by montmorillonite clays). Both clay types will allow for capillary rise to
34 504 sustain the evaporation processes, but their water holding capacities are poor, and
35 505 vertisols display pronounced cracking and swelling, which would negatively affect the
36 506 transpiration process. This explains the pronounced increase in recharge under
37 507 afforestation scenario.

38 508
39 509 The decreased ET was due to the conversion of forest/mixed vegetation to cropland (see
40 510 Table 7, where ET for cropland is marginally smaller than for the other two land uses).
41 511 Zhang *et al.* (2012) indicated that a decrease in forest cover reduces ET from both canopy
42 512 interception and plant transpiration. The results obtained for water yield under the BAU
43 513 (+9.1%) and afforestation (-18%) scenarios are in accordance with other studies such as
44 514 those by De Moraes *et al.* 2006; Coe *et al.* 2009, and Dos Santos *et al.* 2018. For example,
45 515 in the Goseng catchment, Nugroho *et al.* (2013) found that surface runoff and water yield
46 516 (total runoff) increased due to a decrease in vegetation cover. Similarly, other studies such
47 517 as those by Bewket and Sterk (2005) and Costa *et al.* (2003) have confirmed that LULC

1
2
3 517 change such as the conversion of forest to agriculture and urban areas can increase the
4 518 rates of Q_{surf} and groundwater recharge. According to the studies by Andréassian *et al.*
5 519 (2004) and (Brauman *et al.* 2007), a reduced forest coverage leads to an increase in annual
6 520 flow, flood peaks and flood volume. Warburton *et al.* (2012) also noticed that the
7 521 expansion of forest and shrub cover reduces catchment water yields and increases storage
8 522 capacity, which confirms the increase in recharge obtained in this study under
9 523 afforestation scenario. Similarly, López-Moreno *et al.* (2013) showed that an increase in
10 524 forest cover in the Upper Aragón River basin caused a decrease in annual streamflow by
11 525 16%. Indeed, our results also indicated that within the baseline model run, lower surface
12 526 runoff was simulated under forest/mixed vegetation (5.8%) compared to cropland (9.3%)
13 527 and grassland (10.5%) which covers greater part of the study area.
14
15
16
17
18

19 529 The increased forest cover (conversion of cropland to forest/mixed vegetation) under
20 530 afforestation scenario would eventually lead to an increase in evapotranspiration due to
21 531 the increase in water consumption by the trees which increases plant transpiration
22 532 (Oliveira *et al.* 2018). Also, the surface runoff and water yield decreased while recharge
23 533 increased because trees function as a media of water infiltration enhancement into the soil
24 534 through the process of temporary detention of rainwater by interception, stemflow, and
25 535 throughfall which increases the water storage (Nugroho *et al.* 2013). As noted by Li *et al.*
26 536 (2018), a naturally vegetated land has relatively lower water yield coefficients due to
27 537 higher rates of water infiltration. According to Mwangi *et al.* (2016), the ground surface
28 538 roughness increases when forest/mixed vegetation increases, and this also accounts for
29 539 an enhanced infiltration and a decrease in surface runoff generation. Moreover,
30 540 afforestation leads to a reduction of the peak flows over the hydrological year, since it
31 541 increases the infiltration capacity and the effective root zone, thus, increasing storage
32 542 capacity (Wiekenkamp *et al.* 2016; Lamparter *et al.* 2018).
33
34
35
36
37
38

39 544 4 CONCLUSION

40
41 545 The Soil and Water Assessment Tool (SWAT) was configured for the Veá catchment to
42 546 study the water balance components under business-as-usual (BAU) and afforestation
43 547 scenarios of land use by forcing the SWAT model with both station and gridded
44 548 precipitation, and other climatic driving data. The study found that about 74% of the
45 549 rainfall received at the catchment is converted into actual evapotranspiration, and the
46 550 remaining is shared between the other components of the water balance. This partitioning
47 551 is consistent across the three main land use types. **The magnitude of the LULC change
48 552 impact on the water balance components varied, with the greatest difference between the
49 553 two scenarios found for surface runoff. The changes in land use played an important role
50 554 in the water balance, indicated by an increased water yield and surface runoff under the
51 555 BAU scenario; these were decreased under the afforestation scenario. The conversion
52 556 from cropland to forest/mixed vegetation would lead to a decrease in curve number in
53 557 that area hence a decrease in surface runoff and water yield under afforestation scenario.
54 558 On the other hand, the BAU scenario would lead to an increase in catchment curve
55 559 number, hence increased surface runoff and water yield. The study also found that ET**

1
2
3 560 increased under afforestation scenario but decreased under BAU scenario due to higher
4 561 leaf area index of forest/mixed vegetation which is equivalent to the surface area of leaves
5 562 from which moisture can be released (either from an intercepted pool of stored water on
6 563 the leaves, just after rainfall, or via transpiration when leaves are dry). In addition, it was
7 564 found that water loss at the catchment was more influenced by evaporation than
8 565 transpiration (due to the physical properties of the lixisoils and vertisols in this area),
9 566 hence the pronounced increased in recharge under afforestation scenario. From an
10 567 ecosystem service perspective, the increased water yield due to cropland and grassland
11 568 expansion would contribute to the blue water available for consumption but would
12 569 increase soil erosion and flood risks during storms. The increase in groundwater recharge
13 570 under both scenarios of LULC change, especially under afforestation scenario, would
14 571 increase the availability of groundwater resources for different usages in the catchment.
15 572 The insights acquired in this study provide a useful reference relating to the important
16 573 role of land use change in water resources planning and the need for stakeholders and
17 574 policy makers to consider practical trade-offs between changes in water balance
18 575 components and other benefits of afforestation in the small scale Veia catchment.
19 576

20 577 **Acknowledgments** This paper was extracted from Larbi's Doctoral research study
21 578 undertaken at Universite D'Abomey Calavi, Benin. His sincere appreciation goes to the
22 579 Federal Ministry of Education and Research (BMBF) and West African Science Centre
23 580 on Climate Change and Adapted Land Use (WASCAL; www.wascal.org) for providing
24 581 the scholarship and financial support for this programme. Verhoef and Macdonald
25 582 contribution was supported by the BRAVE project (Building understanding of climate
26 583 variability into planning of groundwater supplies from low storage aquifers in Africa),
27 584 funded under the NERC/DFID/ESRC UPGrO Programme (NE/M008983/1 and
28 585 NE/M008827/1). David Macdonald publishes with the permission of the Executive
29 586 Director, British Geological Survey.
30 587

31 588 **Conflicts of Interest:** The authors declare no conflict of interest.
32 589

33 590 REFERENCES

- 34 591
35 592 Abbaspour, K. C. et al. 2009. Assessing the impact of climate change on water resources
36 593 in Iran. *Water resources research*, 45.
37 594 Abbaspour, K.C. 2008. *SWAT Calibration and Uncertainty Programs—A User Manual*;
38 595 Department of Systems Analysis, Integrated Assessment and Modeling (SIAM),
39 596 Eawag, Swiss Federal Institute of Aquatic Science and Technology:
40 597 Duebendorf, Switzerland.
41 598 Adanea, Z. A. et al. 2018. Impact of grassland conversion to forest on groundwater
42 599 recharge in the Nebraska Sand Hills. *Journal of hydrology: Regional studies*,
43 600 15, 171-183.
44 601 Adongo, T. A. et al. 2014. Siltation of the Reservoir of Veia Irrigation Dam in the Bongo
45 602 District of the Upper East Region, Ghana. *International Journal of Science and*
46 603 *Technology*, 2224-3577

- 1
2
3 604 Andréassian, V. 2004. Waters and forests: From historical controversy to scientific
4 605 debate. *J. Hydrol.*, 291, 1–27.
- 6 606 Arnold, J. G. and Allen, P. M. 1993. Bernhardt, G. A comprehensive surface-groundwater
7 607 flow model. *Journal of hydrology*, 142, 47–69.
- 8 608 Arnold, J. G. et al. 1998. Large-area hydrologic modeling and assessment: Part I. Model
9 609 development. *J. American Water Resour. Assoc.*, 34(1): 73-89.
- 11 610 Arnold et al. 2000. Regional estimation of base flow and groundwater recharge in the
12 611 Upper Mississippi River basin. *Journal of Hydrology* 227: 21–40.
13 612 DOI:10.1016/S0022-1694(99)00139-0.
- 15 613 Awotwi, A. et al. 2015. Predicting hydrological response to climate change in the White
16 614 Volta catchment, West Africa. *Journal of Earth Science & Climatic Change*, 6,
17 615 1–7, doi:10.4172/2157-7617.1000249.
- 19 616 Awotwi, A., Yeboah, F., and Kumi, M. 2014. Assessing the Impact of Land Cover and
20 617 Climate Changes on Water Balance Component in White Volta Basin. *Water*
21 618 and Environment journal, doi:10.1111/wej.12100
- 23 619 Baatuuwii, B.N. 2015. *Multi-dimensional approach for evaluating land degradation in*
24 620 *the savanna belt of the White Volta basin*. PhD dissertation, KNUST, Ghana.
- 26 621 Bansode, S. and Patil, K. 2016. Water Balance Assessment using Q-SWAT. *International*
27 622 *Journal of Engineering Research*, Volume, 515–518.
- 28 623 Bewket, W., and Sterk, G. 2005. Dynamics land cover and its effect on the stream flow
29 624 on the Chemoga catchment in the Blue Nile basin, Ethiopia. *Hydrol. Process.*,
30 625 19, 445-458.
- 32 626 Bhaduri, B. et al. 2000. Assessing catchment-scale, long-term hydrologic impacts of land
33 627 use change using a GIS-NPS model, *Environ. Management*, 26(6), 643-658.
- 35 628 Bossa, A. Y. et al. 2014. Scenario-based impacts of land use and climate change on land
36 629 and water degradation from the meso to regional scale. *Water*, 6, 3152–3181,
37 630 doi:10.3390/w6103152.
- 39 631 Braimoh, A.K. and Vlek, P.L.G. 2004. Land-cover change analyses in the Volta Basin of
40 632 Ghana. *Earth Interactions*, 8, p.21.
- 41 633 Brauman, K.A. et al. 2007. The nature and value of ecosystem services: An overview
42 634 highlighting hydrologic services. *Annu. Rev. Environ. Resour.*, 32, 67–98.
- 44 635 Chen, J.M. and Black, T.A. 1992. Defining leaf area for non-flat leaves. *Plant, Cell and*
45 636 *Environment* 15, pp. 421-429.
- 47 637 Coe et al. 2009. The influence of historical and potential future deforestation on the
48 638 stream flow of the Amazon River—Land surface processes and atmospheric
49 639 feedbacks. *J. Hydrol.*, 369, 165–174.
- 51 640 Costa, M. H. et al. 2003. Effects of large-scale changes in land cover on the discharge of
52 641 the Tocantins River, Southeastern Amazonia. *Journal of Hydrology*, 283: 206–
53 642 217.
- 54 643 Dewitte, O. et al. 2013. Harmonisation of the soil map of Africa at the continental scale.
55 644 *Geoderma* 211, 138–153.
- 57 645 Doerr, S. H. et al. 2000. Soil water repellency: its causes, characteristics and hydro
58 646 geomorphological significance, *Earth-Sci. Rev.*, 51, 33–65.

- 1
2
3 647 Dos Santos et al. 2018. Hydrologic Response to Land Use Change in a Large Basin in
4 648 Eastern Amazon. *Water*, MDPI, 10 (4), pp.429, 10.3390/w10040429.halshs-
5 649 01758828
6
7 650 De Moraes et al. 2006. Water storage and runoff processes in plinthic soils under forest
8 651 and pasture in Eastern Amazonia. *Hydrol. Process.* 20, 2509–2526.
9
10 652 Eastman, R.J. 2006. *IDRISI Andes, guide to GIS and image processing*. Clark University,
11 653 Worcester, pp.87-131.
12
13 654 Forkuor, G. 2014. *Agricultural Land Use Mapping in West Africa Using Multi-sensor*
14 655 *Satellite Imagery*. PhD dissertation, Julius-Maximilians-Universität Würzburg
15 656 Friesen, J. et al. 2005. Storage capacity and long-term water balance of the Volta Basin,
16 657 West Africa. IAHS Publication, 296,138-145
17
18 658 Funk, C. et al. 2015. The climate hazards infrared precipitation with stations—a new
19 659 environmental record for monitoring extremes. *Scientific Data* 2, 150066.
20 660 doi:10.1038/sdata.2015.66 2015.
21
22 661 Gassman, P. W. et al. 2007. The soil and water assessment tool: historical development,
23 662 applications, and future research directions. *Transactions of the ASABE*, 50,
24 663 1211–1250.
25
26 664 Ghoraba, S. M. 2015. Hydrological modeling of the Simly Dam catchment (Pakistan)
27 665 using GIS and SWAT model. *Alexandria Engineering Journal*, 54, 583–594.
28
29 666 Guug, S. 2017. *Modelling Water Balance and Availability with Swat Hydrological Model*
30 667 *of the Sherigu catchment in the Upper Region of Ghana. Master's MSc Thesis,*
31 668 *I*, 1–110.
32
33 669 Hargreaves, G., and Samani Z. A. 1985. Reference crop evapotranspiration from
34 670 temperature, *Applied engineering in agriculture* 1: 96–99.
35
36 671 Ibrahim B. et al. 2015. Hydrological predictions for small ungauged watersheds in the
37 672 Sudanian zone of the Volta basin in West Africa *Journal of Hydrology: Regional*
38 673 *Studies* 4 (2015) 386–397
39
40 674 Jones, J. R. et al. 2015. Temporal variability of precipitation in the Upper Tennessee
41 675 Valley. *Journal of Hydrology: Regional Studies*, 3, 125–138.
42
43 676 Kankam-Yeboah, K. et al. 2013. Impact of climate change on streamflow in selected river
44 677 basins in Ghana. *Hydrological sciences journal*, 58, 773–788,
45 678 doi:10.1080/02626667.2013.782101.
46
47 679 LAMPARTER, G. et al.2018. Modelling hydrological impacts of agricultural expansion
48 680 in two macro-catchments in Southern Amazonia, Brazil. *Regional*
49 681 *Environmental Change*, v. 18, n. 1, p. 91-103.
50
51 682 Larbi, I. et al. 2018. Spatio-Temporal Trend Analysis of Rainfall and Temperature
52 683 Extremes in the Veia Catchment, Ghana. *Climate*, 6, 87; doi:10.3390/cli6040087
53
54 684 Larbi, I. et al. 2019. Predictive Land use change under business as usual and afforestation
55 685 scenarios in the Veia Catchment, West Africa, *International Journal of*
56 686 *Advanced Remote Sensing and GIS*, 7, Volume 8, Issue 1, pp. ISSN 2320 –
57 687 0243, DOI: <https://doi.org/10.23953/cloud.ijarsg.416>.
58
59 688 Li et al. 2018. Impacts of Land-Use and Land-Cover Changes on Water Yield: A Case
60 689 Study in Jing-Jin-Ji, China. *Sustainability*, 10, 960.

- 1
2
3 690 Limantol, A. M. et al. 2016. Farmers' perception and adaptation practice to climate
4 691 variability and change: a case study of the Veua catchment in Ghana.
5 692 *SpringerPlus*, 5, 830, doi:10.1186/s40064-016-2433-9.
6
7 693 López-Moreno, J.I., et al. 2013. Impact of climate and land use change on water
8 694 availability and reservoir management: Scenarios in the Upper Aragón River,
9 695 Spanish Pyrenees. *Science of the Total Environment* 493, 1222–
10 696 1231. doi.org/10.1016/j.scitotenv.2013.09.031
11
12 697 Mango L. M. et al. 2010. Land use and climate change impacts on the hydrology of the
13 698 upper Mara River Basin, Kenya: results of a modeling study to support better
14 699 resource management. *Hydrol Earth Syst Sci*, 15: 2245–2258.
15
16 700 Martin, N. 2005. *Development of a water balance for the Atankwidi catchment, West*
17 701 *Africa - A case study of groundwater recharge in a semi-arid climate*. Doctoral
18 702 thesis. University of Göttingen
19
20 703 Mohamed, E. R. 2010. Impacts and Implications of Climate Change for the Coastal Zones
21 704 of Egypt. Delta., 31–50.
22
23 705 Moriasi, D.N. et al. 2007. Model evaluation guidelines for systematic quantification of
24 706 accuracy in catchment simulations. *Trans. ASABE*, 50 (3), 885–900.
25
26 707 Mwangi, H.M. et al. 2016. Modelling the impact of agroforestry on hydrology of Mara
27 708 River Basin in East Africa. *Hydrological Processes*, 30(18), 3139-3155.
28 709 <https://doi.org/10.1002/hyp.10852>
29
30 710 Nash, J. E. and Sutcliffe, J.V. 1970. River Flow forecasting through conceptual models.
31 711 Part I: A discussion of principles. *J. Hydrol.*, 10:282-290
32
33 712 Neitsch, S. L. et al. 2011. *Soil and water assessment tool theoretical documentation*
34 713 *version 2009*; Texas Water Resources Institute
35
36 714 Neitsch, S., Arnold, J., Kiniry, J., and Williams, J. 2005. Soil and Water Assessment Tool
37 715 theoretical documentation - version 2005. *Grassland, Soil & Water Research*
38 716 *Laboratory, Agricultural Research Service, and Blackland Agricultural*
39 717 *Research Station, Temple, TX*, 1–12.
40
41 718 Nugroho et al. 2013. Impact of land-use changes on water balance. *Procedia*
42 719 *Environmental Sciences*, 17, 256 – 262.
43
44 720 Obuobie, E. 2008. *Estimation of groundwater recharge in the context of future climate*
45 721 *change in the White Volta River Basin*. PhD dissertation, Rheinische Friedrich
46 722 Wilhelms Universität, Bonn/ Germany.
47
48 723 Oguntunde, P., 2004. Evapotranspiration and complimentary relations in the water
49 724 balance of the Volta Basin: field measurements and GIS-based regional
50 725 estimates. In: PhD Thesis, Ecology and Development Series No. 22. Cuvillier
51 726 Verlag, Göttingen http://www.zef.de/fileadmin/webfiles/downloads/zefcecology_development/ecol_dev_22_text.pdf
52 727
53
54 728 Oliveira, V.A. et al. 2018. Land-use change impacts on the hydrology of the upper grande
55 729 river basin, Brazil. *CERNE*, v. 24, n. 4, p. 334-343.
56
57 730 Olmedo, et al. 2015. Comparison of simulation models in terms of quantity and allocation
58 731 of land change. *Environ. Model. Softw*, 69, pp.214-221.
59
60 732 Palazzoli, I. et al. 2015. Impact of prospective climate change on water resources and
733 crop yields in the Indrawati basin, Nepal. *Agricultural Systems*, 133, 143–157.

- 1
2
3 734 Santhi, C. et al. 2001. Validation of the swat model on a large rwer basin with point and
4 735 nonpoint sources. *JAWRA Journal of the American Water Resources*
5 736 *Association*, 5, 1169–1188.
- 7 737 Schuol, J., and Abbaspour, K. C. 2007. Using monthly weather statistics to generate daily
8 738 data in a SWAT model application to West Africa. *Ecological modelling*, 201,
9 739 301–311.
- 11 740 Shawul, A. A., Alamirew, T., and Dinka, M. O. 2013. Calibration and validation of
12 741 SWAT model and estimation of water balance components of Shaya
13 742 mountainous catchment, Southeastern Ethiopia. *Hydrology and Earth System*
14 743 *Sciences Discussions*, 13955–13978.
- 16 744 Sivasena, A. R and Janga, M. R. 2015. Evaluating the influence of spatial resolutions of
17 745 DEM on watershed runoff and sediment yield using SWAT. *J. Earth Syst.*
18 746 *Sci.*124, No. 7, pp. 1517–152
- 20 747 Sloan, P.G. and Moore, I.D. 1984. Modelling subsurface stormflow on steeply sloping
21 748 forested watersheds. *Water Resour. Res.*, 20, 1815–1822.
- 23 749 Soil Conservation Service Engineering Division (SCSD).1986. *Urban Hydrology for*
24 750 *Small Watersheds*; Technical Release 55; U.S. Department of Agriculture:
25 751 Washington, DC, USA.
- 27 752 Stackhouse, P. W. et al. 2018. POWER Release 8 (with GIS Applications) Methodology
28 753 (Data Parameters, Sources, & Validation) Documentation (Data Version 8.0.1)
29 754 <https://power.larc.nasa.gov/data-access-viewer/>
- 31 755 Stonestrom, D. A., Scanlon, B. R., and Zhang, L. 2009. Introduction to special section on
32 756 Impacts of Land Use Change on Water Resources. *Water Resour. Res.*, 45,
33 757 W00A00, doi:10.1029/2009WR007937.
- 35 758 Tang, Z. et al. 2005. Forecasting land use change and its environmental impact at a
36 759 catchment scale, *J. Environ. Manage.*, 76, 35-45.
- 37 760 Vilaysane, B. et al. 2015. Hydrological stream flow modelling for calibration and
38 761 uncertainty analysis using SWAT model in the Xedone river basin, Lao PDR.
39 762 *Procedia Environmental Sciences*, 28, 380–390.
- 41 763 Wang, N. L. et al. 2015. Variations of the glacier mass balance and lake water storage in
42 764 the Tarim Basin, northwest China, over the period of 2003–2009 estimated by
43 765 the ICESatGLAS data. *Environ. Earth Sci.*, 74, 1997–2008.
- 45 766 Warburton M.L, Schulze R.E., and Jewitt G.P.W. 2012. Hydrological impacts of land use
46 767 change in three diverse South African catchments. *J Hydrol*;4 14–415:118–35.
- 48 768 Wei, X. H., Liu, W. F., and Zhou, P. C. 2013. Quantifying the Relative Contributions of
49 769 Forest Change and Climatic Variability to Hydrology in Large Catchments: A
50 770 Critical Review of Research Methods. *Water*, (5) 728-746.
- 52 771 WIEKENKAMP, I. et al.2016 Spatial and temporal occurrence of preferential flow in a
53 772 forested headwater catchment, *Journal of Hydrology*, v. 534, n. 1, p. 139-149.
- 54 773 Winchell, M., Srinivasan, R., Di Luzio, M., and Arnold, J. 2013. Arcswat Interface for
55 774 Swat 2012; User Guide. Temple, Texas: Agricultural Experiment Station and
56 775 Agricultural Research Service, US Department of Agriculture.

- 1
2
3 776 Yin, Z. et al. 2016. Assessing variation in water balance components in mountainous
4 777 inland river basin experiencing climate change. *Water*, 8, 472, doi:
5 778 10.3390/w8100472.
6
7 779 Yira, Y. et al. 2017. Modeling land use change impacts on water resources in a tropical
8 780 West African catchment (Dano, Burkina Faso). *J. Hydrol.* 537, 187–199.
9 781 doi:https://doi.org/10.1016/j.jhydrol.2016.03.052
10
11 782 Zhang, L., Zhao, F.F., and Brown, A.E. 2012. Predicting effects of plantations expansion
12 783 on streamflow regime for catchments in Australia. *Hydrology and Earth System*
13 784 *Sciences* 16: 2109-2121.
14
15 785 Zhang, S. et al. 2008. Recent changes of water discharge and sediment load in the
16 786 Zhujiang (Pearl River) Basin, *China. Glob Planet Chang*, 60, 365-380.
17
18
19
20
21
22
23
24
25
26
27
28
29
30
31
32
33
34
35
36
37
38
39
40
41
42
43
44
45
46
47
48
49
50
51
52
53
54
55
56
57
58
59
60

Table 1. Datasets used within the SWAT modelling of the Veia Catchment and their sources

S/N	Data type	Description	Source
1	DEM	30m digital elevation model for delineation of the catchment boundary, stream networks and sub-catchments.	Shuttle Radar Topography Mission (SRTM) http://earthexplorer.usgs.gov/
2	Climate	Daily rainfall (mm), maximum and minimum temperature (°C) from 1990-2017.	Ghana Meteorological Agency, WASCAL Veia catchment, CHIRPS and NASA POWER
3	Hydrological	Daily discharge data from 2013-2015 from Sumbrugu river gauging station for calibration and validation of SWAT model.	WASCAL Veia catchment
4	Soil map/properties	10km soil map, Soil texture and physical properties such as: bulk density, hydrological group, available water content, hydraulic conductivity and organic matter content for two layers (30cm and 100cm) for the three soil types namely; lixisols (Lf1-1a), vertisols (Vc1) and cambisols (Bv2) in Figure 2.	CSIR-Soil Research Institute (Ghana), Harmonized World Soil Database (Dewitte <i>et al.</i> , 2013).
5	Land use/land cover map	LULC map of the year 2016	Landsat image classification (Larbi <i>et al.</i> 2019)

Table 2. Land use/ land cover classification scheme used for the Veia Catchment after Larbi *et al.* (2019)

LULC Categories	Description
Water bodies	Areas permanently covered with standing or moving water such as inland waters, water logged areas, wetlands, dams, dugouts, and streams.
Grassland	Mainly mixture of grasses and shrubs with or without scattered trees (<10 trees per hectare) areas covered with only grasses.
Built-Up areas	Areas of human settlements, roads, artificial surfaces etc.
Cropland	Areas used for crop cultivation (irrigated and rain-fed agriculture), harvested agricultural land and bare soil.
Forest/Mixed Vegetation	Areas with dense trees usually over 5m tall, riparian vegetation, shrub and trees.

Table 3. Distribution of 2016 land use/cover classes within the Veia catchment (Larbi *et al.* 2019)

LULC type	Redefined LULC according to SWAT database	SWAT Code	Area (km ²)	Area Coverage (%)
Cropland	Agricultural Land-Generic	AGRL	174.50	56.64
Grassland	Range Grass	RNGE	82.72	26.85
Built-Up Areas	Residential	URBN	1.67	0.54
Water Bodies	Range-Grasses	WATR	4.90	1.59
Forest/Mixed Vegetation	Forest Mixed	FRST	44.28	14.37

Table 4. Current and 2025 LULC area statistics (in km²) in the Veia catchment

LULC Class	Baseline 2016	2025 scenarios	
		BAU	Afforestation
Cropland	174.50 (56.6%)	177.04 (57.5%)	155.5 (51.3%)
Grassland	82.72 (26.8%)	88.06 (28.5%)	94.55 (31.3%)
Built-Up Areas	1.67 (0.5%)	1.67 (0.5%)	1.02 (0.5%)
Water Bodies	4.90 (1.6%)	4.90 (1.6%)	4.90 (1.6%)
Forest/Mixed Vegetation	44.28 (14.4%)	36.40 (11.8%)	46.66 (15.3%)

Note: The areas expressed as percentages areas of the total area are in brackets.

Table 5. Input parameters and bounds, sensitivity ranking and calibrated values by the SWAT model for the Veia catchment

Parameters	Definition	Lower/upper bounds	Calibrated values	Sensitivity Rank
HRU_SLP	Average slope steepness (m/m)	0.0-1.0	0.014	1
V_CN ₂ .mgt_AGRL	Curve number for cropland,	35-90	72.5	2
V_CN ₂ .mgt_RNGE	Curve number for grassland		73.5	
V_CN ₂ .mgt_FRST	Curve number for forest/mixed vegetation.		69.0	
V_ALPHA_BF.gw	Baseflow alpha factor (days)	0.0-1.0	0.02	3
V_ESCO.hru	Soil evaporation compensation factor	0.0-1.0	0.42	4
R_REVAPMN.gw	Threshold depth of water in shallow aquifer for revap to occur	0.0-1000	550	5
SLSUBBSN.hru	Average slope length (m)	10-150	121.9	6
V_GWQMN.gw	Threshold depth of water in the shallow aquifer for return	0.0-5000	2200	7

1
2
3
4
5
6
7
8
9
10
11
12
13
14
15
16
17
18
19
20
21
22
23
24
25
26
27
28
29
30
31
32
33
34
35
36
37
38
39
40
41
42
43
44
45
46
47
48
49
50
51
52
53
54
55
56
57
58
59
60

		flow to occur (mm)		
R_EPCO.hru	Plant uptake compensation factor	0.0-1.0	0.02	8
V_GW_REVAP.gw	Groundwater “revap” coefficient.	0.02-0.2	0.02	9
V_GW_DELAY.gw	Groundwater delay (days)	0- 500	33	10
R_GW_SPYLD.gw	Specific yield of the shallow aquifer (m ³ /m ³)	0.0-0.4	0.003	11
SURLAG.bsn	Surface runoff lag time (days)	0.0-24	2	12
R_RCHRG_DP.gw	Deep Aquifer percolation coefficient	0.0- 1.0	0.25	13
BLAI_AGRL	Maximum LAI for cropland	0.5-10	3	
BLAI_RNGE	Maximum LAI for grassland	0.5-10	2.5	
BLAI_FRST	Maximum LAI for forest/mixed vegetation	0.5-10	5	
RDMX_AGRL	Maximum rooting depth (m) for cropland	0-4	1	
RDMX_RNGE	Maximum rooting depth (m) for grassland	0-4	1	
RDMX_FRST	Maximum rooting depth (m) for forest/mixed vegetation	0-4	3	

R: parameter value is multiplied by 1+given value; V: parameter value is replaced by the calibrated value

Table 6. Mean annual water balance components simulated by SWAT under different land use/cover types at catchment scale

LULC	rainfall (mm)	Q_surf (mm)	Q _{gw} (mm)	ET (mm)
Cropland	949.3	88.5(9.3%)	50.5 (5.6%)	700.5 (72.9%)
Forest/mixed vegetation	972.87	56.2(5.8%)	74.3 (7.7%)	720.1 (74.0%)
Grassland	951.45	100.3(10.5%)	37.9 (4.0%)	698.8 (73.4%)

NB: Percentage rainfall contribution between brackets

Table 7. Mean annual water balance components under 2016 and 2025 LULC change scenarios over the simulated period (1993-2017)

Water balance components	Baseline (2016)	BAU Scenario	afforestation scenario
Rainfall (mm)	954.5	954.5	954.5
Actual evapotranspiration, ET (mm)	709.5	689.8(-2.7%)	714 (+0.6%)
Surface runoff, Q_Surf (mm)	82.5	97.9(+18.7%)	66.3 (-19.6%)
Water yield, WYLD (mm)	128.4	140.3 (+9.1%)	105.1(-18.0%)
Groundwater recharge (mm)	115.1	132.8(+15.3%)	147.4 (+28.1)

NB: Values in brackets indicate percentage change in water balance component relative to the baseline for each scenario

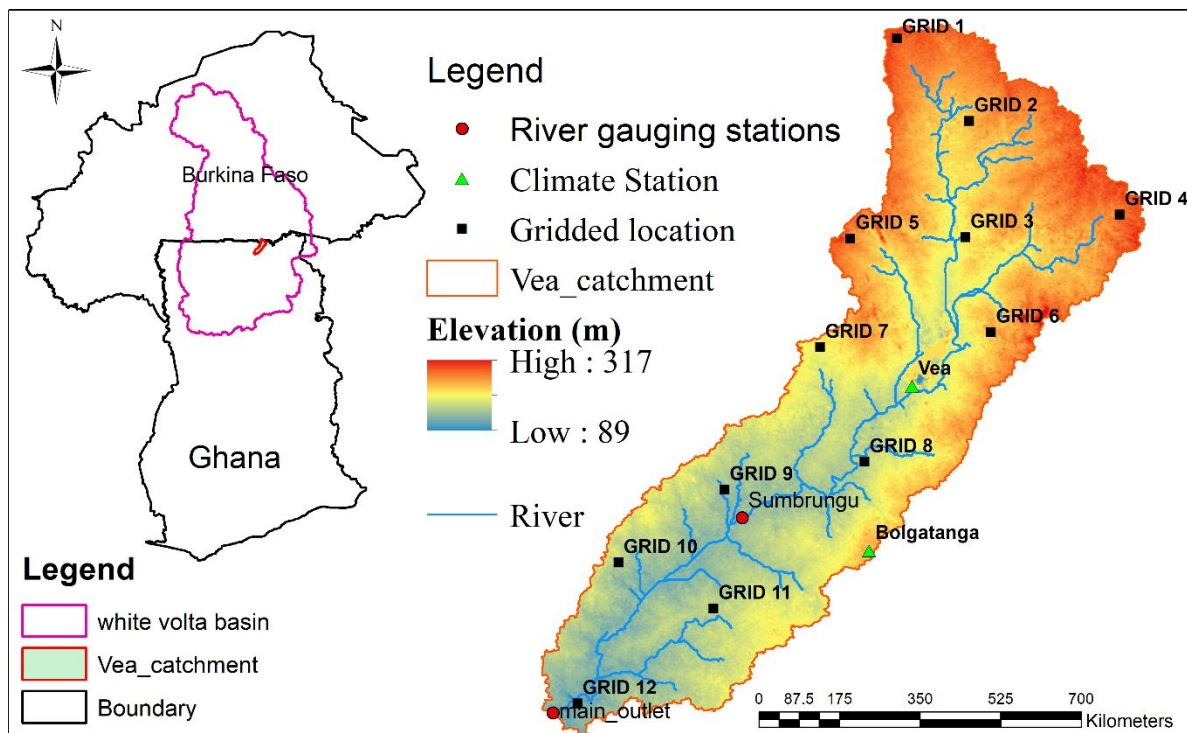


Figure 1 Location of the Veja catchment within the White Volta Basin, as well as the topography, weather and hydrological measurement stations in the Veja catchment, after Larbi et al. (2018).

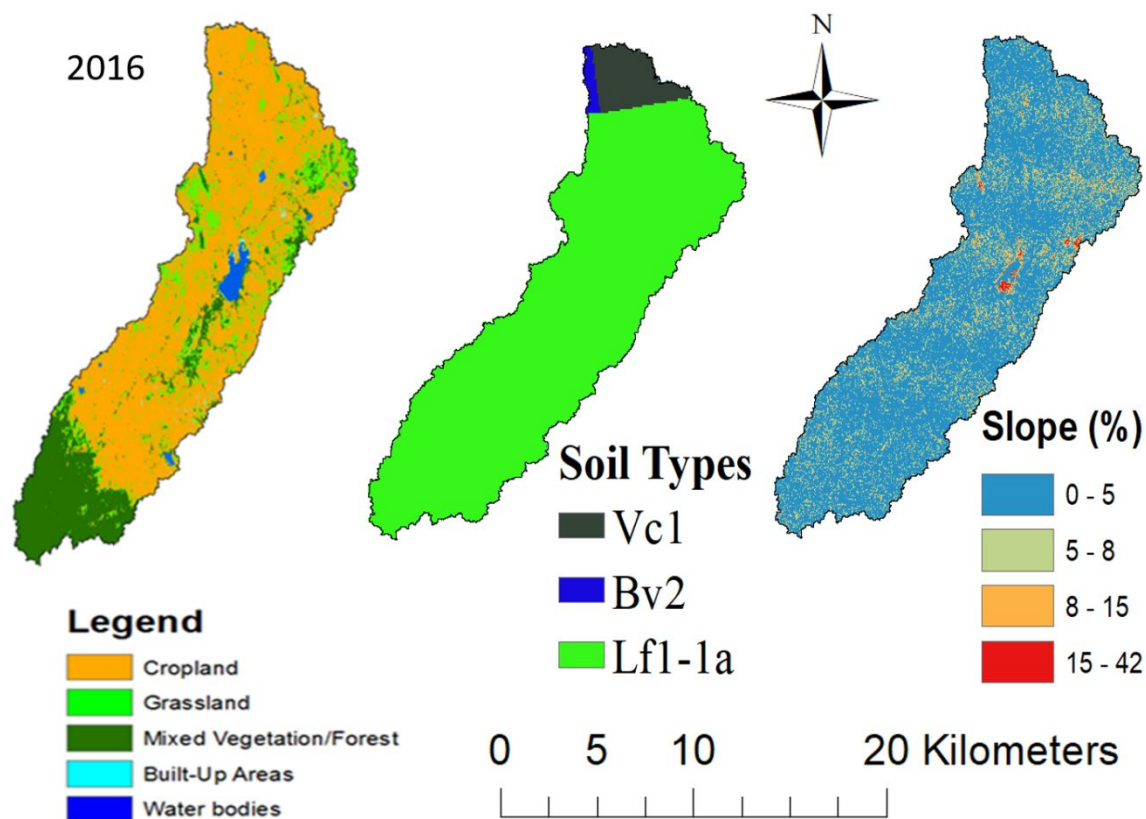


Figure 2 Land use/land cover (left), Soil (middle), and slope classes (right) maps of the Veja catchment. Lixisols (Lf1-1a), vertisols (Vc1) and cambisols (Bv2)

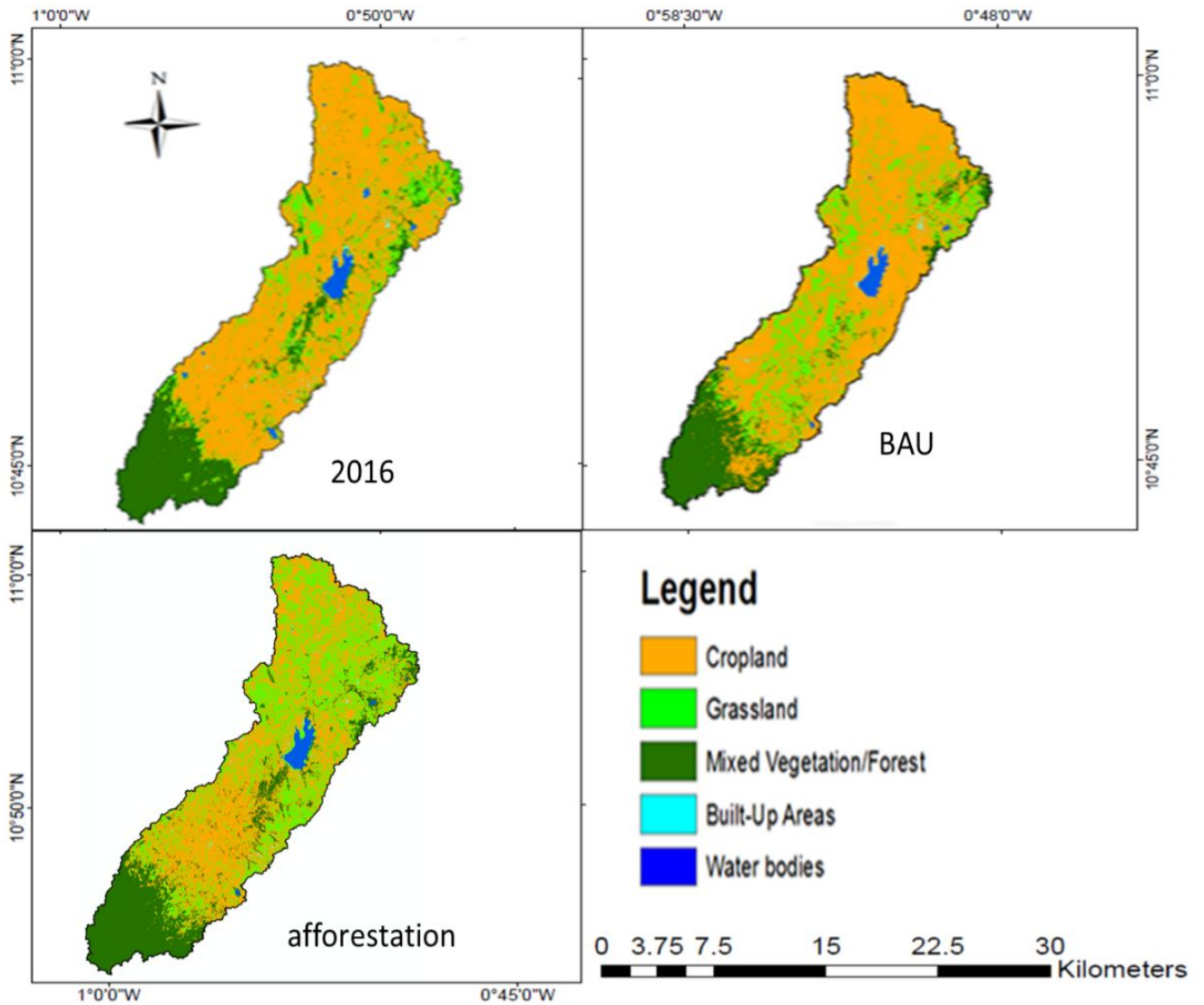


Figure 3 The baseline and 2025 LULC change scenarios maps of the Veia catchment (Larbi et al. 2019)

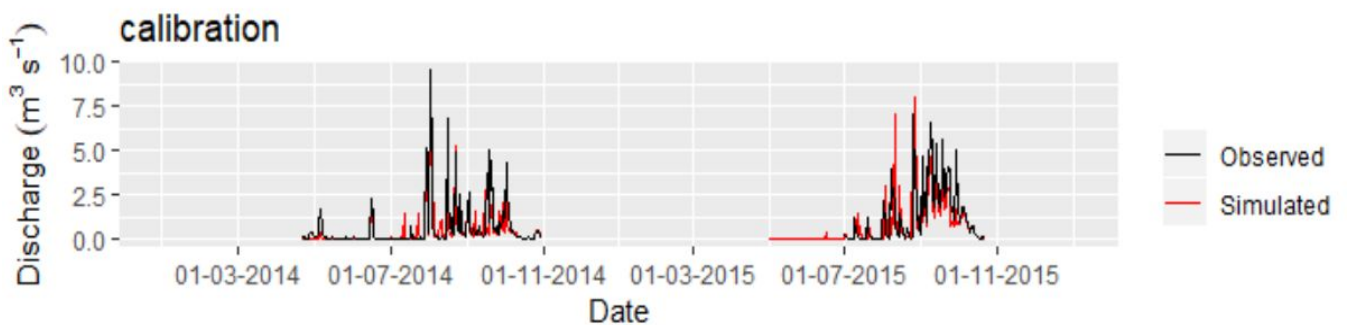


Figure 4 Simulated vs. Observed daily discharge for *calibration* period (2014-2015) at Sumbrungu gauge station, Veia Catchment

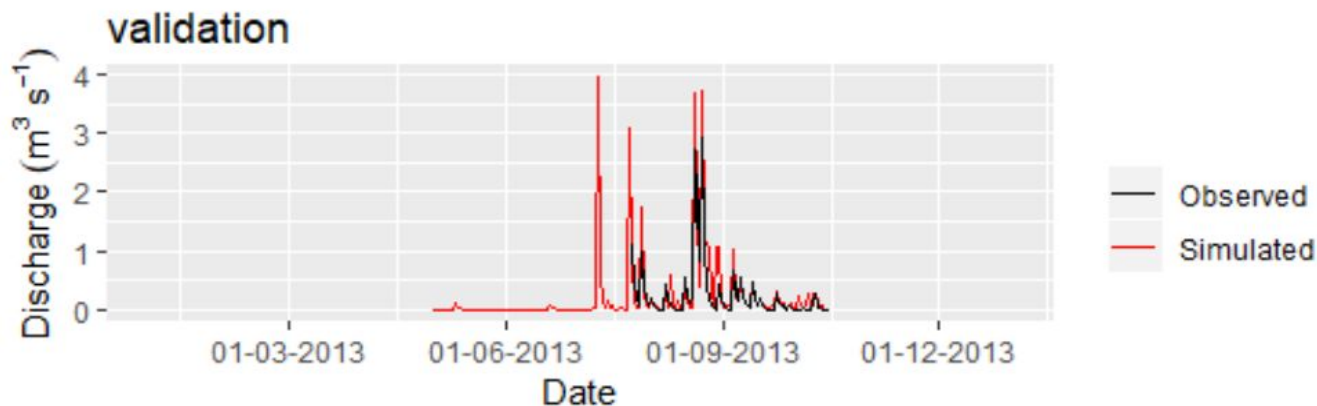


Figure 5 Simulated vs. Observed daily discharge for validation period (2013) for Sumbrungu gauge station, Vea Catchment

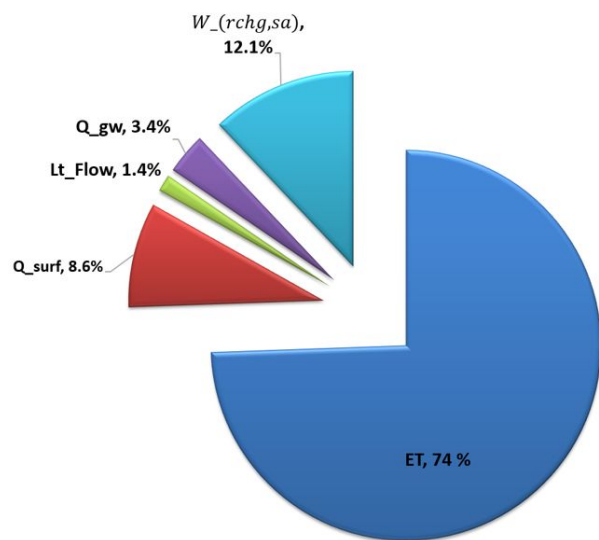


Figure 6: Mean annual water balance components as a proportion of rainfall for the Vea catchment. Q_{surf} , ET , Lt_{flow} , Q_{gw} , and $W_{(rchg,sa)}$ are surface runoff, actual evapotranspiration, lateral flow, groundwater flow, shallow aquifer recharge respectively.

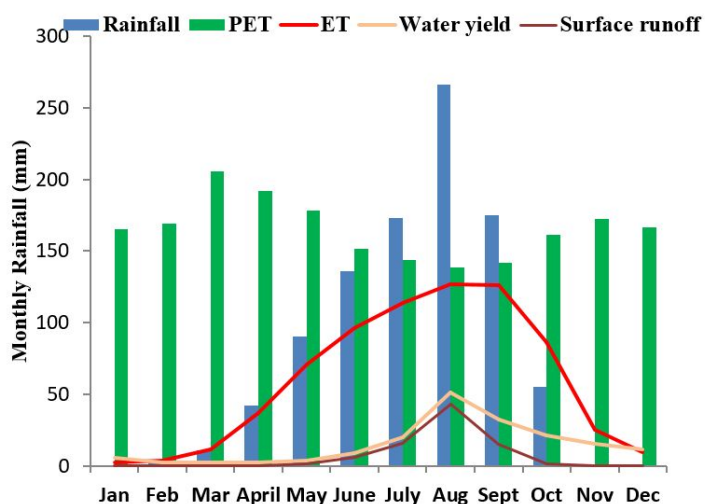


Figure 7: Mean monthly water balance components from 1993-2017 for the Vea catchment.

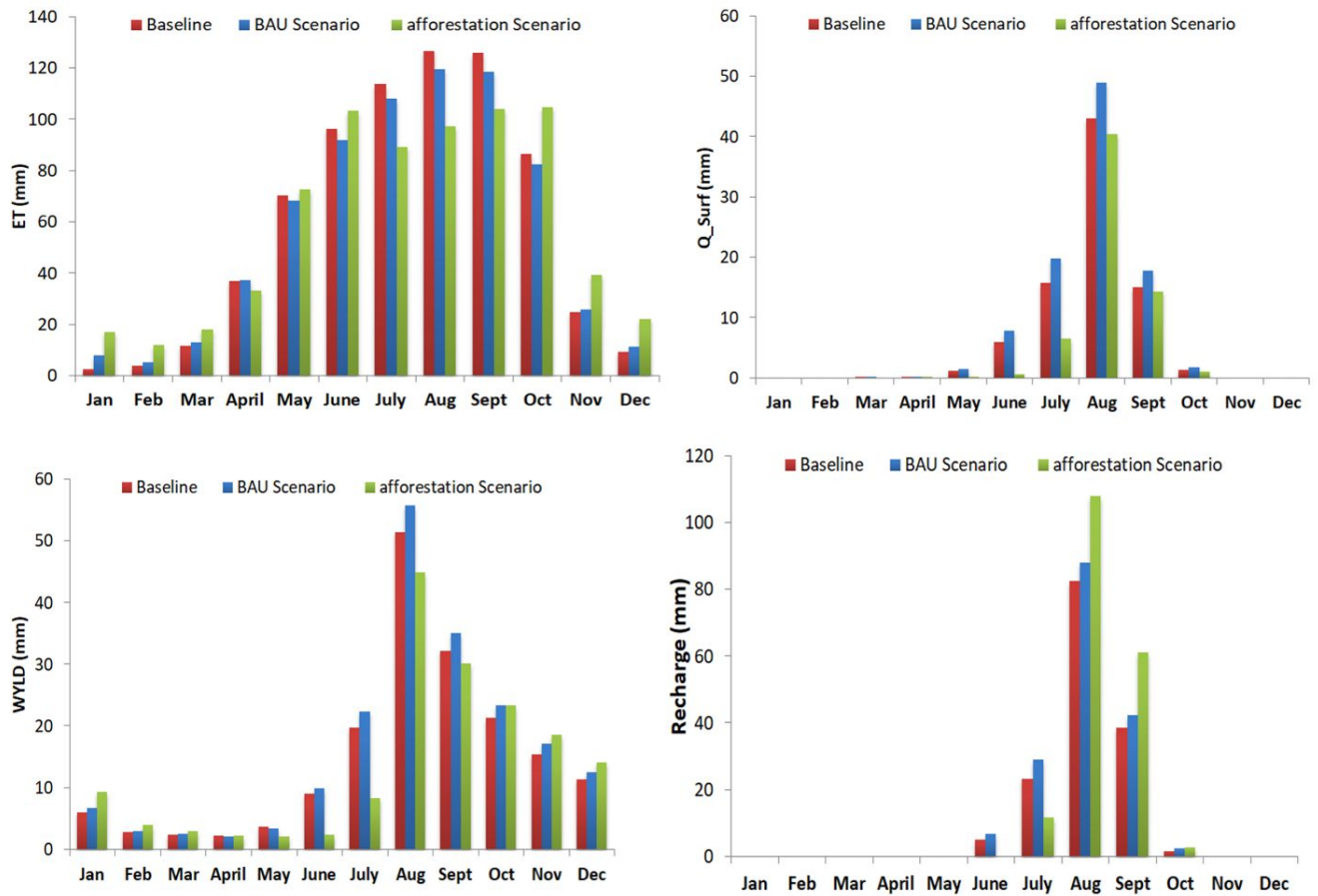


Figure 8 Mean monthly water balance components under different scenarios of land use change

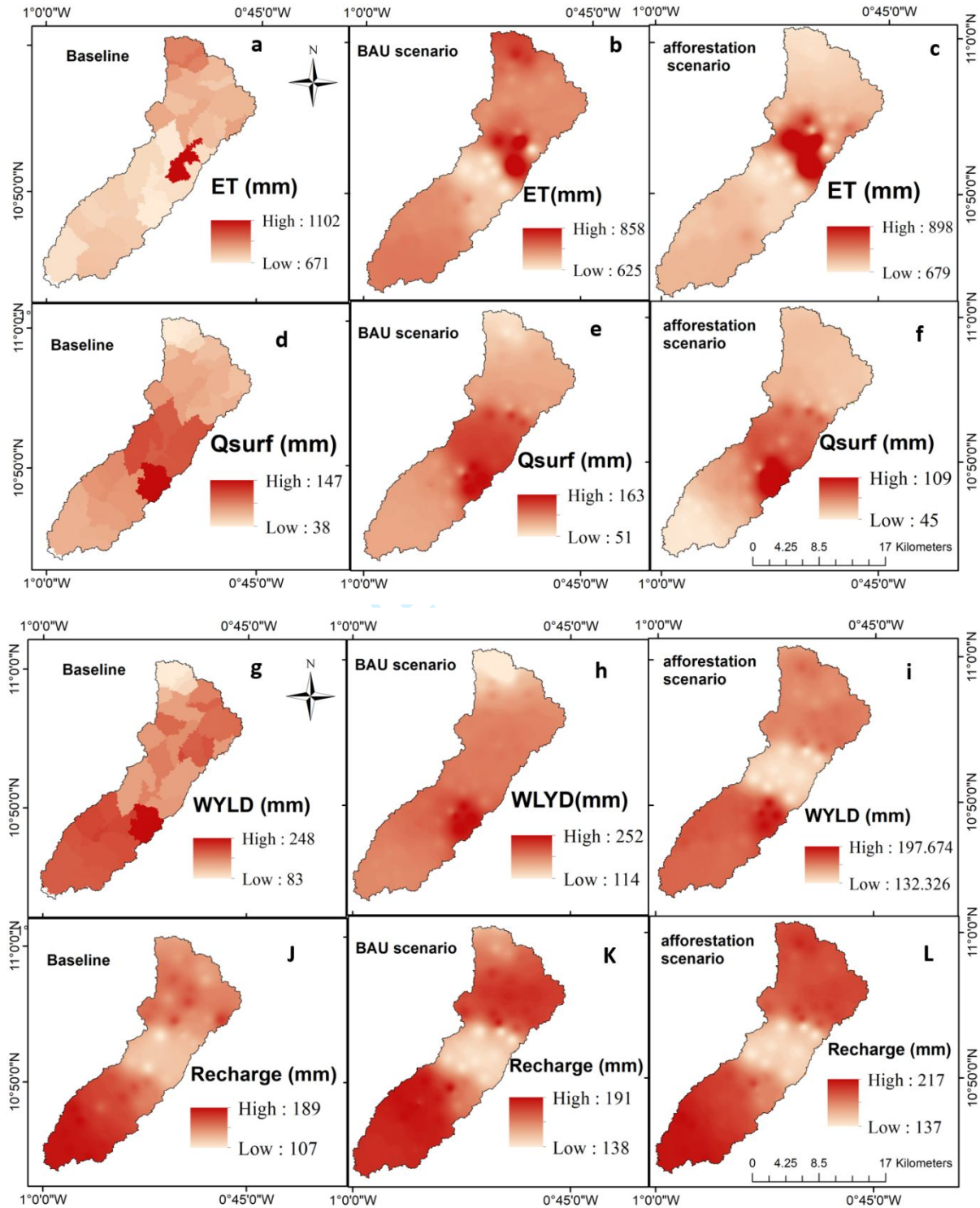


Figure 9 SWAT Simulated mean annual water balance components under BAU and afforestation scenarios of land use change relative to the baseline (2016) LULC map